

Pulse-read on erasable thermal phase-change superresolution disks

Jia-Reuy Liu, Pei-Yih Liu, Nai-Yuan Tang, and Han-Ping D. Shieh

New erasable thermal phase-change superresolution (EPSR) disks composed of mask and recording layers can increase recording density by the detection of the below-diffraction-limited marks within the readout spot. The formation of the aperture and the readout signal on the EPSR disk were analyzed. The feasibility of optically designed EPSR disks was evaluated by thermal simulation. A carrier-to-noise ratio of 32 dB at a mark size of 0.4 μm , 8 dB higher than that of a conventional disk, was obtained by application of a pulse-read method to the EPSR disks at a wavelength of 780 nm and a numerical aperture of 0.55. © 1998 Optical Society of America

OCIS codes: 210.0210, 210.4590, 210.4810.

1. Introduction

Erasable phase-change materials are being considered for use as such high-density optical data-storage media as DVD-RAM. Compared with the capacity of 4.7 Gbytes of the first-generation DVD video¹ disk, the 2.6-Gbyte capacity of the proposed first-generation DVD-RAM² disk is not enough to record a 133-min high-quality movie. Moreover, the capacity needed for recording a 133-min high-resolution HDTV movie is as much as 15 Gbytes. Therefore increased recording density is essential for the development of higher-density and thus higher-capacity DVD-RAM disks as primary storage media in a multimedia era.

The recording density of optical disks is restricted by the optical diffraction limit. Although using a short-wavelength laser diode and a high numerical-aperture (NA) lens can increase the recording density by reduction of the spot size of the focused laser, lenses with NA's greater than 0.6 and blue laser diodes are still expensive and are not readily available. Therefore methods to increase the recording density, such as zone constant-angular velocity, pulse-width modulation, land-groove recording,³ and superresolution,^{4,5} have been proposed. The principle of su-

perresolution is to form an equivalent readout aperture within a diffraction-limited reading spot; thus the recording density can be increased greatly at a given laser wavelength and objective NA. The magnetic superresolution^{4,5} method has already been applied to erasable magneto-optical recording to increase the capacity of a 3.5-in. disk to 7 Gbytes.^{6,7} However, the technique of superresolution by use of phase-change media has been reported only for read-only disks.^{8,9}

In this paper a new structure for an erasable phase-change disk that uses the superresolution detection method is proposed. Analyses of the readout signal of erasable phase-change superresolution (EPSR) disks were made by optical simulation^{10,11}; the possibility of effective detection on EPSR disks was evaluated by thermal analysis. According to the simulation results, the EPSR disk structure was designed to yield adequate signal readout by use of an appropriate readout aperture.

In contrast to the dc read method used for conventional phase-change disk readout, we applied a pulse-read^{12,13} method to detect the signal on the EPSR disks. We show the advantages of using pulse-read on the EPSR disks to achieve higher recording density by exploring its feasibility analytically and experimentally.

2. Principle

The mechanism for detecting below-diffraction-limited marks in a thermal phase-change superresolution disk is related to the refractive index of the phase-change material as a function of temperature. When the temperature of the phase-change material

The authors are with the Institute of Electro-Optical Engineering, National Chiao Tung University, Hsinchu 30010, Taiwan. H.-P. D. Shieh's e-mail address is hpshieh@cc.nctu.edu.tw.

Received 9 February 1998; revised manuscript received 26 August 1998.

0003-6935/98/358187-08\$15.00/0

© 1998 Optical Society of America

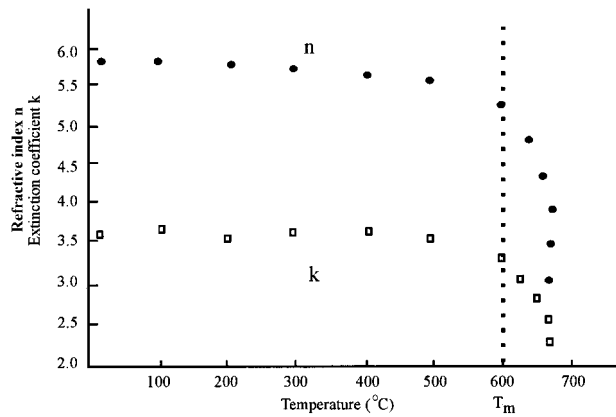


Fig. 1. Refractive index of the phase-change material as a function of temperature (from Ref. 5). T_m is the melting temperature.

is above the melting temperature T_m , both the real (n) and the imaginary (k) parts of the index of refraction decrease rapidly, as illustrated in Fig. 1. The sharp temperature variations in n and k had previously been used in a ROM disk to achieve superresolution optically.^{8,9}

To facilitate a similar sharp temperature variation in the index of refraction, we propose the use of a new EPSR disk containing a mask layer and a recording layer, as sketched in Fig. 2. The mask layer and the recording layer of the EPSR disk are both composed of phase-change media consisting of germanium (Ge), tellurium (Te), and antimony (Sb) but in different ratios and therefore with different critical cooling rates.¹⁴ The three dielectric layers are all composed of ZnS-SiO₂. The main functions of the middle dielectric layer are to prevent material diffusion between the mask and the recording layers and to control the cooling rate of the mask layer. The upper and the lower dielectric layers are used to control the reflection coefficient of the EPSR disk and the cooling rate of the recording layer, respectively. An aluminum (Al) layer functions as a heat sink and a reflective layer.

The ability to detect below-diffraction-limited marks on the EPSR disks is a result of the difference between the refractive indices of the mask and the recording layers near the melting temperature. The amorphous marks and the nonrecorded crystalline

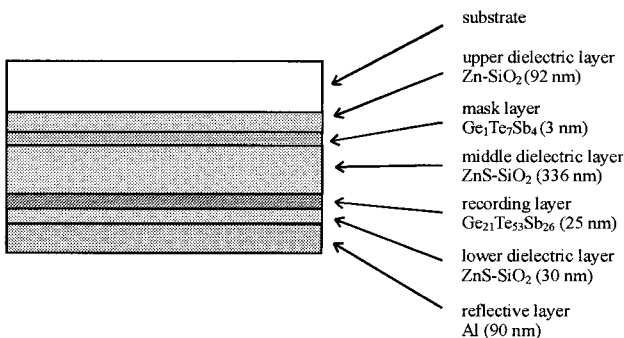


Fig. 2. Structure of the new EPSR disk.

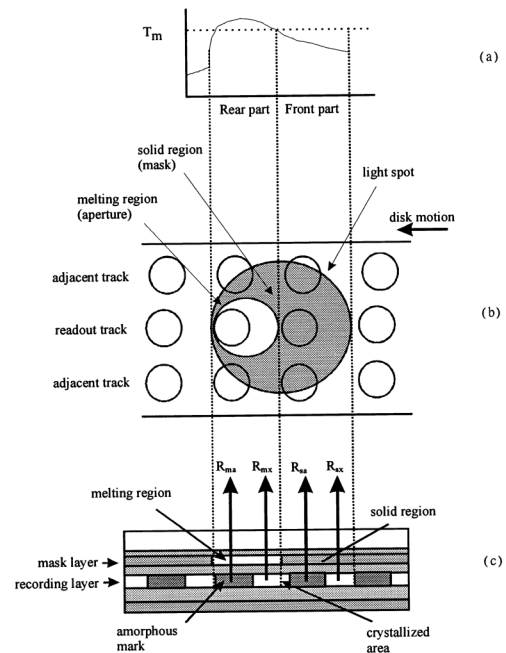


Fig. 3. Principle of the EPSR disk: (a) Temperature profile of the mask layer when a light spot scans to read out a track. (b) Aperture and mask regions formed on the EPSR disk. (c) Reflection coefficients R_{ma} , R_{mx} , R_{sa} , and R_{sx} within a light spot.

area of the recording layer have different refractive indices. When the light spot scans the readout track, the temperatures of the rear part and the front part of the mask layer inside the light spot are above and below the melting point T_m , respectively, as shown in Fig. 3(a), and also correspond to two different refractive indices, as depicted in Fig. 1. Therefore there are four reflection coefficients, R_{ma} , R_{mx} , R_{sa} , and R_{sx} , within a light spot, as shown in Figs. 3(b) and 3(c). In the melting region of the mask layer, R_{ma} and R_{mx} denote the reflection coefficients when the recording layer is in an amorphous and a crystalline state, respectively; in the solid region of the mask layer, R_{sa} and R_{sx} denote the reflection coefficients when the recording layer is in an amorphous and a crystalline state, respectively, as illustrated in Fig. 3(c). In rear-aperture detection (RAD), the melting region (the rear part of the light spot) and the solid region (the front part of the light spot) of the mask layer are designed to be the aperture and the mask regions of the diffraction-limited reading spot, respectively; however, in front-aperture detection (FAD) the solid region (the front part of the light spot) and the melting region (the rear part of the light spot) of the mask layer function as aperture and mask, respectively. If the RAD method is adopted, the reflection coefficients R_{ma} and R_{mx} and the contrast ratio $(R_{mx} - R_{ma})/R_{mx}$ within the thermal aperture should be designed to be higher than those in the mask area. As a result, the contrast ratio within the thermal aperture will be the principal determinant of the signal modulation of the reading spot; in contrast, $(R_{sx} - R_{sa})/R_{sx}$ in the mask area will result in noise in the readout.

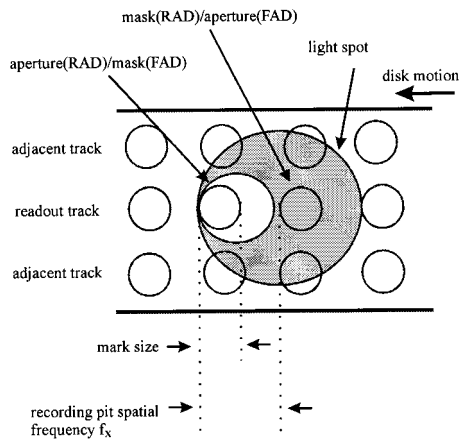


Fig. 4. Circular aperture and crescent mask in RAD at the rear and the front parts, respectively, of the light spot; in contrast, the crescent aperture and the circular mask in FAD are at the front and the rear parts, respectively, of the light spot.

The nonsymmetric temperature profile caused by the dynamic scanning of the reading spot on the readout track¹⁵ is, in fact, favorable for the formation of an appropriate detection aperture and mask in an EPSR disk. Careful material selection and layer thickness design permit the formation of the melting aperture and the solid mask regions for detection of below-diffraction-limited marks. Moreover, the critical cooling rate of the mask layer should be designed to be higher than that of the recording layer; thus amorphous marks are recorded only in the recording layer and not in the mask layer.

3. Optical Simulation

We derived the simulated readout signal $S(t)$ of EPSR disks by taking the convolution of the Gaussian profile of a diffraction-limited light spot, $L(x, y)$, and the distribution of data marks, $R(x, y)$, in the track:

$$S(t) = \iint L[x(t), y]R[X(t) - x(t), y]dx dy. \quad (1)$$

The wavelength and the NA in the simulation were 650 nm and 0.6, respectively; thus the calculated full width at half-maximum ($\sim 0.6\lambda/\text{NA}$) of the light spot was approximately 0.64 μm . The mark size and the spatial frequency of the recorded pit employed in the simulation were 0.25 ($0.6\lambda/\text{NA}$), or 0.16 μm , and 0.5 ($0.6\lambda/\text{NA}$), or 0.32 μm , respectively; in other words, a light spot covered two pit periods, as shown in Fig. 4. The carrier-to-noise ratio (CNR), or power spectrum $P(f)$, of readout signal $S(t)$ then can be derived by Fourier transformation of $S(t)$:

$$P(f) = \int S(t)\exp(-j2\pi tf)dt. \quad (2)$$

The apertures in RAD and in FAD were circular and crescent shaped, respectively, as shown in Fig. 4; thus cross talk can be introduced by the marks in the adjacent tracks when the FAD method is used,

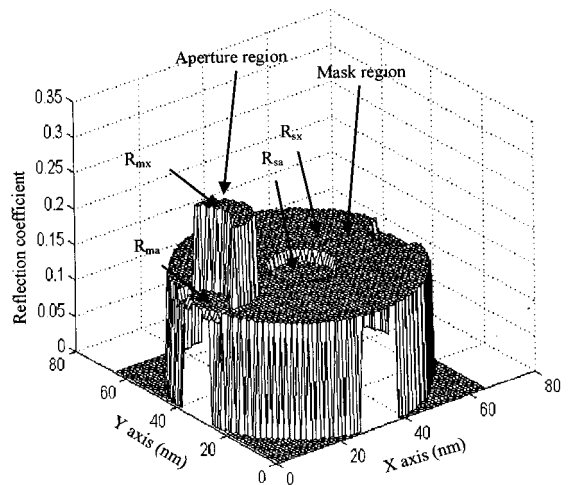


Fig. 5. Reflection-coefficient profiles of RAD in an EPSR disk. The mark size and the light-spot size are 16 and 0.64 μm , respectively. R_{ma} , R_{mx} , R_{sa} , and R_{sx} are 0.154, 0.270, 0.143, and 0.158, respectively.

whereas the RAD method does not do this.¹² Therefore the readout signal for RAD is less noisy than with FAD.

The simulated reflection-coefficient pattern $R(x, y)$ of an EPSR disk composed of ZnS-SiO₂(92 nm)/Ge₁Te₇Sb₄(3 nm)/ZnS-SiO₂(336 nm)/Ge₂₁Te₅₃Sb₂₆(25 nm)/ZnSiO₂(30 nm)/Al(90 nm) detected by RAD is shown in Fig. 5; R_{ma} , R_{mx} , R_{sa} , and R_{sx} are 0.154, 0.270, 0.143, and 0.158, respectively. The calculated results achieved the requirements defined in Section 2: Reflection coefficient R_{mx} in the RAD aperture region is higher than R_{sa} and R_{sx} in the RAD mask region; moreover, the contrast ratio of 43% in the aperture region is also higher than that in the mask region. The convolution of the Gaussian profile of the diffraction-limited light spot and $R(x, y)$ at a given time are shown in Fig. 6. The maximum intensity of the Gaussian profile was normalized to 1; therefore the values of readout signal intensity are

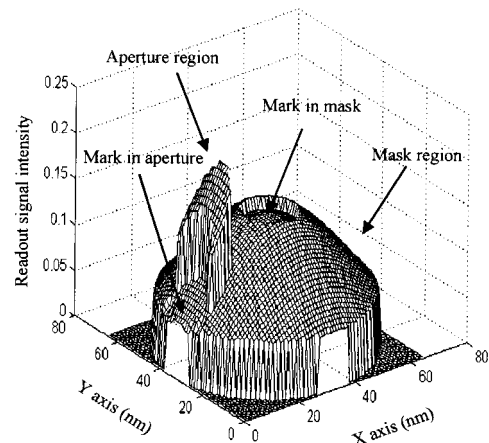


Fig. 6. Convolution of the Gaussian profile of the diffraction-limited light spot and $R(x, y)$.

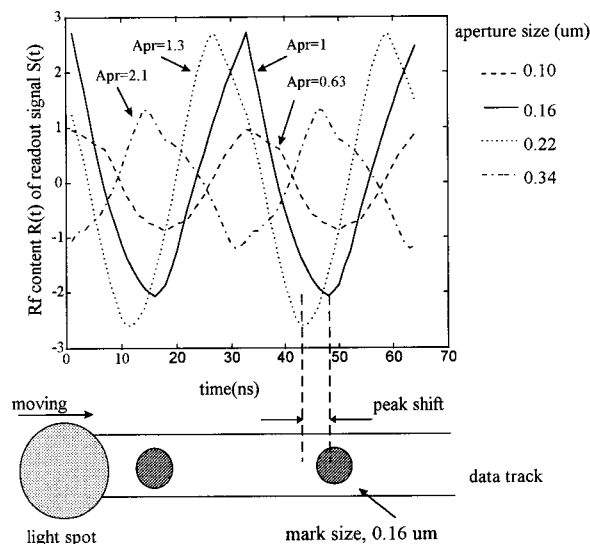


Fig. 7. $r(t)$ of RAD as a function of aperture size. The mark size and the light-spot size are 0.16 and $0.64 \mu\text{m}$, respectively. The aperture size–mark size is defined as the aperture ratio Apr . The maximum $r(t)$ was found at an Apr of 1.3 .

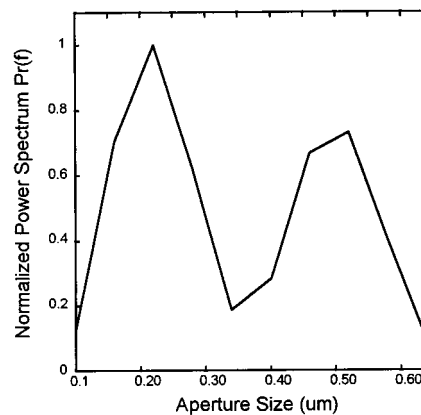
less than those of the reflection coefficients shown in Fig. 5.

The rf content $r(t)$ of the readout signal $S(t)$ in RAD for various sizes of thermal apertures was calculated, and the results are shown in Fig. 7. When the aperture ratio Apr , defined as aperture size:mark size, was smaller or much larger than 1, the amplitude of $r(t)$ was very small (Apr of 0.63 or 2.1 in Fig. 7). The maximum readout signal $r(t)$ was found at an Apr of 1.3 , but the peak of $r(t)$ was shifted 18% relative to the mark position. The peak shift was due to the Gaussian distribution of the light-spot intensity. In contrast, the amplitude of $r(t)$ at an Apr of 1 was 10% lower than at an Apr of 1.3 , but there was no peak shift. Thus Apr 's of 1.3 and 1 may be suitable for use in pulse-position modulation and pulse-width modulation, respectively.

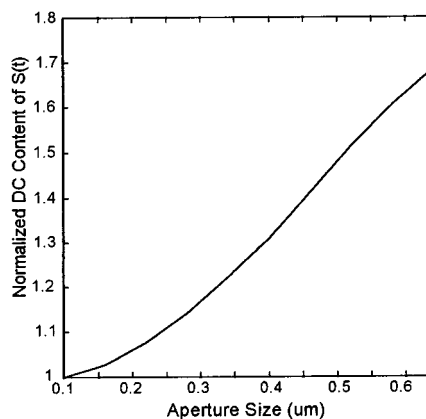
The power spectrum $Pr(f)$ of $r(t)$ at various aperture sizes was derived with the fast Fourier transform, and the results are shown in Fig. 8(a). The maximum $Pr(f)$ appeared at an aperture size of $0.22 \mu\text{m}$, corresponding to an Apr of 1.3 . As the aperture size increased to $0.52 \mu\text{m}$, $Pr(f)$ increased to 80% of the maximum $Pr(f)$; however, the dc content of $S(t)$ also increased by 1.5 times, as shown in Fig. 8(b). As a result, the incremental increase in aperture size decreased the modulation depth, defined as the $Pr(f)/\text{dc}$ content of $S(t)$, and then caused difficulty in differentiating the rf signal from noise. Accordingly, we adopted an aperture size smaller than the pit period for use in the detection of the readout signal $S(t)$ in the EPSR disks.

4. Thermal Simulation

The feasibility of optically designed EPSR disks was evaluated by a thermal simulation. The thermal properties of the thin-film layers used for the calcu-



(a)



(b)

Fig. 8. (a) Normalized power spectrum $Pr(f)$ of $r(t)$ as a function of the aperture size. (b) The dc content of the readout signal $S(t)$ as a function of the aperture size.

lations are listed in Table 1. In the reading analysis of the EPSR disks, the readout laser light was modeled as a Gaussian-distributed light beam. The allocation of laser energy within the disk structure was simulated by a thin-film theorem and metrics.^{17,18} After the laser light was absorbed in the mask layer and the recording layer of the EPSR disks, the temperature profiles were analyzed by three-dimensional dynamic heat-diffusion equations.¹⁵

The aperture wall, defined as a transition region of the refractive index from the melting point T_m to the readout temperature T_r in the mask layer, as shown in Fig. 9, affects the quality of the readout signal of

Table 1. Thermal Properties of EPSR Disk Layers Used for Our Calculations^a

Thin-Film Material	Thermal Conductivity ($\text{J cm}^{-1} \text{K}^{-1} \text{s}^{-1}$)	Specific Heat ($\text{J cm}^{-3} \text{K}^{-1}$)
ZnS–SiO ₂	0.0658	2.044
Ge ₁ Te ₇ Sb ₄	0.0058	1.285
Ge ₂₁ Te ₅₃ Sb ₂₆	0.0058	1.292
Al	2.144	2.448

^aSource, Ref. 16.

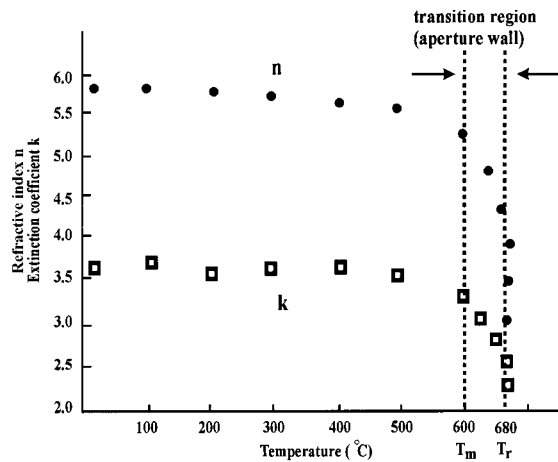


Fig. 9. The aperture wall, which is a transition region of the refractive index in the mask layer from melting point T_m (T_m) to readout temperature T_r (T_r).

the EPSR disks. To achieve effective reading–recording on the EPSR disks without destroying the recorded amorphous marks, we had to obey certain criteria: (1) In reading, the temperature of the mask layer had to be higher than the readout temperature T_r of the phase-change materials to form the readout aperture; in contrast, that of the recording layer had to be kept below the crystallization temperature T_x to avoid erasing the amorphous marks. (2) In recording, the temperature of the recording layer had to be higher than the melting point T_m , and the cooling rate of the recording layer had to be high enough to form amorphous marks; meanwhile, the cooling rate of the mask layer had to be low enough to avoid the formation of amorphous marks.

A dc laser beam scanning along a track of a disk is usually used for readout in conventional disks. However, the wall width of the readout aperture in the mask layer becomes too thick because of heat diffusion by application of a dc read method to the EPSR disks to yield an adequate CNR, as shown in Fig. 10(a). Furthermore, when the temperature of the mask layer of the recording layer exceeded T_r , the temperature of the recording layer exceeded T_x ; thus the amorphous marks in the recording layer were erased, as shown in Fig. 10(b). The read power P_r and the linear velocity used in the dc readout thermal simulation were 5.5 mW and 5 m/s, respectively. Alternatively, use of pulse–read could form a melting aperture with a thinner aperture wall and prevent erasure of amorphous marks in the recording layer. The simulated results showed that the maximum temperature of the recording layer was lower than T_x and the wall width of the readout aperture was reduced to 30% of that in dc read, as shown in Figs. 11(a) and 11(b), respectively. The pulse width and the high–low–power levels of the reading pulse used in the thermal simulation were 50 ns and 6–2 mW, respectively. As a result, we adopted the pulse–read method to read out below-diffraction-limited marks on the EPSR disks.

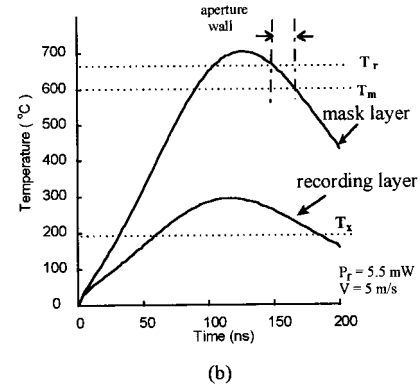
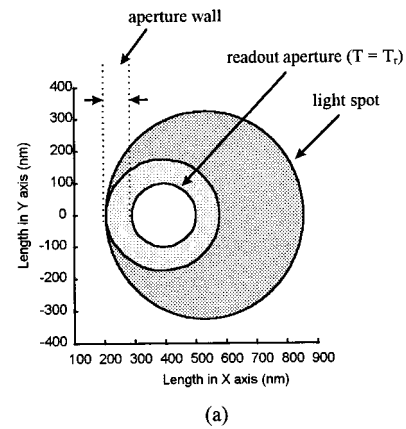


Fig. 10. dc read detection of an EPSR disk. T_m and T_x were the melting and the crystallization temperatures, respectively. (a) Isothermal contour of the mask layer. The isothermal temperature of the readout aperture is T_m . (b) Temperature versus time for the recording and the mask layers. The read power P_r and the linear speed V are 5.5 mW and 5 m/s, respectively.

5. Experiment and Discussion

The EPSR disks contain two layers of phase-change materials: a mask layer composed of $\text{Ge}_1\text{Te}_7\text{Sb}_4$ with a high critical speed of crystallization and a recording layer composed of $\text{Ge}_{21}\text{Te}_{53}\text{Sb}_{26}$ with a low critical speed of crystallization. We determined the characteristics of the two phase-change materials used in the mask and the recording layers by measuring two conventional, four-layer erasable phase-change disks with the same structure but with different recording-layer materials,¹⁹ $\text{Ge}_1\text{Te}_7\text{Sb}_4$ (disk A) and $\text{Ge}_{21}\text{Te}_{53}\text{Sb}_{26}$ (disk B). The measurement conditions were the following: the laser wavelength and the NA were 780 nm and 0.55, respectively; therefore the diffraction-limited spot size was 0.85 μm . The writing power P_w and the bias power P_b were 12 and 6 mW, respectively, the read power P_r was 2 mW, and the linear velocity and the duty cycle were 5 m/s and 30%, respectively.

The CNR of disk A fell below 5 dB, whereas the CNR of disk B remained higher than 23 dB at a writing frequency of 7 MHz, as shown in Fig. 12. The mark size of the disk B recording at 7 MHz was

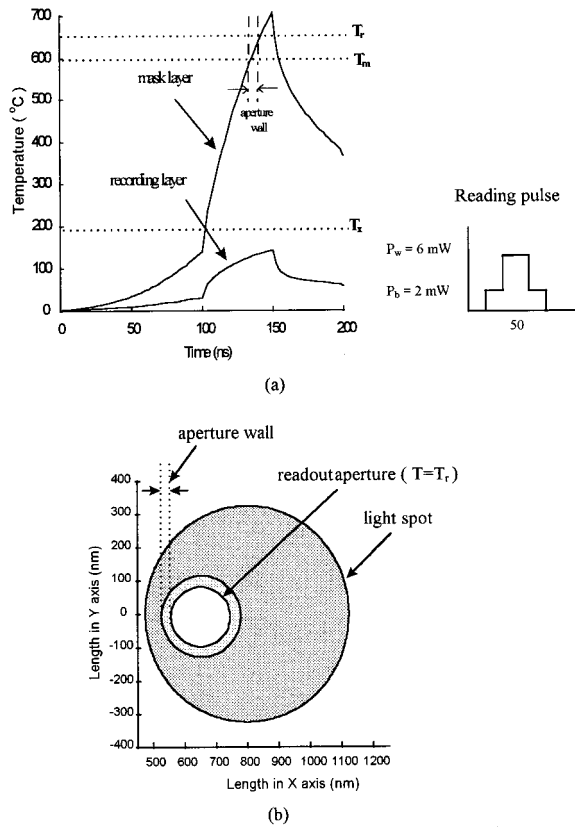


Fig. 11. Pulse-read detection of an EPSR disk. The pulse width and P_w/P_b of the reading pulse are 50 ns and 6/2 mW, respectively; the linear velocity is 5 m/s. (a) Temperature versus time at the recording and the mask layers. (b) Isothermal contour on the mask layer.

0.4 μm , approximately half of the diffraction-limited spot size as measured by a time-interval analyzer. The low CNR at a frequency of 7 MHz in disk A was due to the high critical crystallization speed of $\text{Ge}_1\text{Te}_7\text{Sb}_4$, whereas the detectable CNR of disk A at a frequency lower than 7 MHz might be ascribed to the high cooling rate in the center of the Gaussian-distributed light spot; thus the amorphous marks

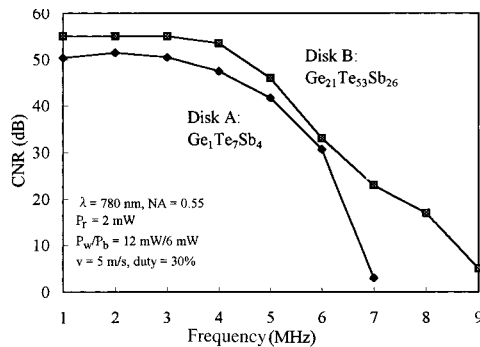


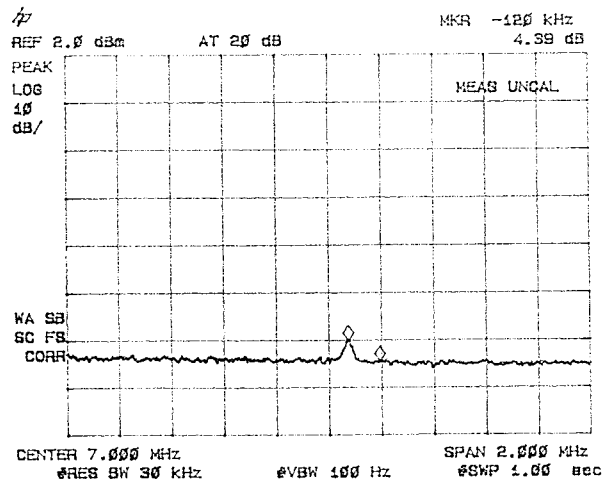
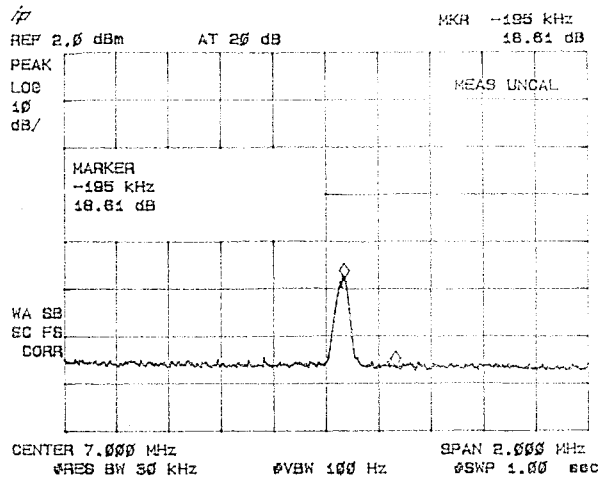
Fig. 12. Recording performance of the phase-change materials used in the mask and the recording layers determined by measurement of two conventional four-layer erasable phase-change disks with the same structure but with different recording-layer materials, $\text{Ge}_1\text{Te}_7\text{Sb}_4$ and $\text{Ge}_{21}\text{Te}_{53}\text{Sb}_{26}$.

were still formed in disk A. The CNR of disk B is still higher than 20 dB at a frequency of 8 MHz because of the low critical cooling rate of $\text{Ge}_{21}\text{Te}_{53}\text{Sb}_{26}$. Therefore $\text{Ge}_1\text{Te}_7\text{Sb}_4$ (the recording layer of disk A) and $\text{Ge}_{21}\text{Te}_{53}\text{Sb}_{26}$ (the recording layer of disk B) were used as the mask and the recording layers, respectively, in the EPSR disk.

The EPSR disks designed by optical and thermal simulation at a wavelength of 780 nm and a NA of 0.55 were tested at a writing frequency of 7 MHz with a below-diffraction-limited mark size of 0.4 μm . The writing and the erasing powers were 12 and 6 mW, respectively, and the linear velocity was 5 m/s. When the conventional dc read detection was utilized, the measured CNR of the tested track in the EPSR disk was 18 dB at a P_r of 2 mW, as shown in Fig. 13(a). Because the dc read power of 2 mW could not form a melting aperture on the mask layer as in the thermal simulation, the measured CNR was ascribed to the formation of an incomplete amorphous mark upon the mask layer. When an erasing power of 3 mW was applied to the same tested track, only the amorphous marks on the mask layer were crystallized, and the CNR was then reduced to 4 dB at a P_r of 2 mW, as shown in Fig. 13(b). In contrast, the recorded marks in the recording layer were not crystallized by the dc read power of 3 mW. Consequently, the residual CNR of 4 dB after 3-mW erasure was caused by the small contrast ratio ($R_{sx} - R_{sa})/R_{sx}$ with no aperture formed in the readout spot and was the main source of noise in EPSR disks.

We analyzed the formation of the melting readout aperture by employing the pulse-read method. We used a reading pulse of 14 MHz, double the signal frequency on the tested track, to avoid confusion between the signal frequency (7 MHz) and the reading frequency (14 MHz). The pulse width and the high (low) power level of the reading pulse in the measurement were 50 ns and 6 (2) mW, respectively. Applying a fast Fourier transform to the readout signal measured by the digital oscilloscope resulted in the appearance of two peaks in the power spectrum of the EPSR disks: One was the signal frequency of 7 MHz on the recording layer and the other was the laser pulse frequency of 14 MHz, as shown in Figs. 14(a) and 14(b), respectively. The measured CNR of the below-diffraction-limited mark size of 0.4 μm on the EPSR disks that resulted from use of the pulse-read method was 32 dB, 8 dB higher than the CNR in the conventional single-recording-layer phase-change disk, as shown in Fig. 15.

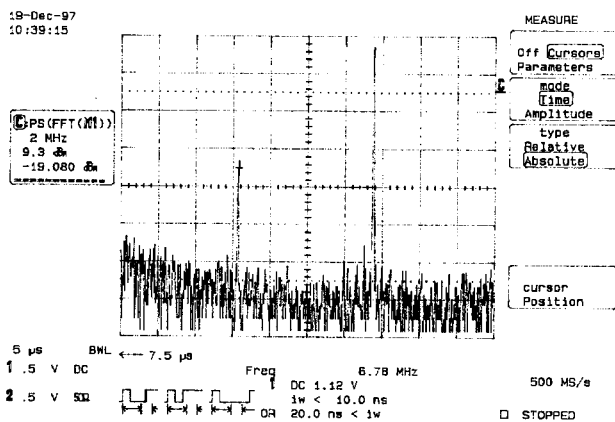
From the difference between the CNR measured with the dc read and the pulse-read methods, a thermal readout aperture formed on the mask layer of the EPSR disks, in agreement with the thermal simulation. Compared with that of the conventional single-recording-layer disk, the CNR of the below-diffraction-limited mark size of 0.4 μm on the EPSR disk was 8 dB higher, confirming that the below-diffraction-limited aperture was formed by use of the superresolution technique, which also agreed with



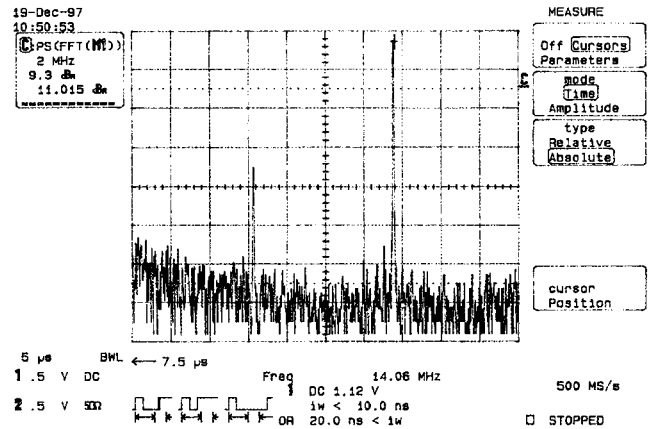
(a)

(b)

Fig. 13. (a) Measured CNR of the EPSR disk written at a frequency of 7 MHz and read out at a P_r of 2 mW. (b) Residual CNR after an erasing power of 3 mW was applied at the same tested track. This was the main source of noise in the EPSR disks.



(a)



(b)

Fig. 14. Fast Fourier transform of the signal measured by application of the pulse-read method to the EPSR disks. (a) The measuring marker at a writing frequency of 7 MHz. (b) The measuring marker at reading frequency of 14 MHz.

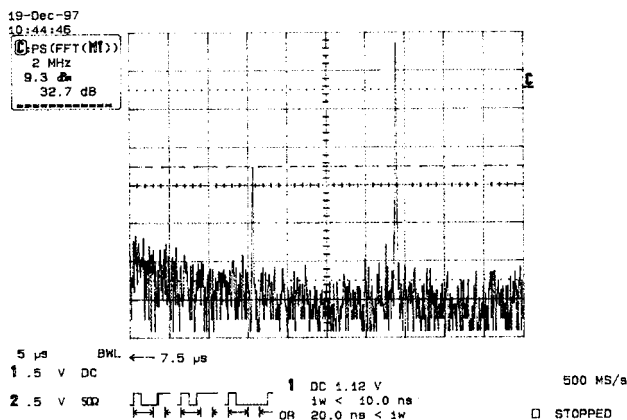


Fig. 15. CNR of 32 dB measured at a mark size of $0.4 \mu\text{m}$ on the EPSR disks by the pulse-read method.

the optical simulation. According to the optical simulation described in Section 2, the minimum mark size is $0.25 (0.6\lambda/\text{NA})$. When a laser wavelength of 780 nm and a NA of 0.55 were used, the detectable minimum mark size on the EPSR disk was reduced to $0.21 \mu\text{m}$, i.e., a pit length of $0.42 \mu\text{m}$, which was the same as the minimum pit length of the DVD-ROM disk of 4.7 Gbytes obtained with a laser wavelength of 650 nm and a NA of 0.6. If 650 nm and a NA of 0.6 were used in reading the EPSR disks, the capacity increased by 1.6 times, i.e., to 7.52 Gbytes in an EPSR disk; therefore the recording density of the erasable phase-change disk could be greatly increased.

To permit practical use of EPSR disks, we are making improvements on them: (a) Another heat-sink layer is being added to control the temperature pro-

file of the mask layer; therefore the thickness of the aperture wall can be reduced, thus reducing noise. (b) The contrast ratios in the aperture and the mask region within the readout spot are being further increased and decreased, respectively; thus the CNR can increase further. (c) The aperture position and size are being properly controlled to gain maximum signal modulation without peak shift. These techniques for the increment of the CNR on the EPSR disks are proceeding both experimentally and analytically, and we intend to publish the results.

5. Conclusion

A new erasable phase-change disk structure that comprises mask and recording layers composed of different phase-change materials with different critical cooling rates has been proposed for use in forming a below-diffraction-limited aperture. An erasable phase change superresolution disk can be designed according to optical and thermal simulations. In the optical model, the structure of the EPSR disk has been derived, and the effect of readout aperture size on the readout signal has been evaluated. In the thermal model the feasibility of EPSR disks designed by optical simulation has been evaluated based on a temperature profile. Moreover, the differences between dc read and pulse-read detection have also been studied. To form a sharp temperature gradient upon the mask layer of the EPSR disk, we used pulsed laser reading to form a well-defined submicrometer detecting aperture. Using a laser wavelength of 780 nm and an objective lens of 0.55 NA, we obtained a CNR of 32 dB at a mark size of 0.4 μm on the EPSR disk by the pulse-read method, 8 dB higher than that in a conventional disk. Therefore the feasibility of applying the super-resolution method to erasable phase-change optical disks has been confirmed, which allows the density and thus the capacity of erasable phase-change disks to increase.

This research was supported by the National Science Council, Republic of China, under contract NSC 87-2622-E009-006.

References

1. Philips, Inc., "Philips and Sony proposed specifications for high density multimedia compact disk," press release (Philips, Inc., Amsterdam, The Netherlands, 16 December 1994).
2. Toshiba, Inc., "DVD specifications for random-access disk," device handbook (Toshiba, Inc., Tokyo, September 1997).
3. N. Miyagawa, Y. Gotoh, E. Ohno, K. Nishiuchi, and N. Akahira, "Land and groove recording for high track density on phase-change disks," *Jpn. J. Appl. Phys.* **32**, 5324–5328 (1993).
4. M. Kaneko, K. Aratani, A. Fukumoto, and S. Miyaoka, "IRISTER—magneto-optical disk for magnetically induced super resolution," *Proc. IEEE* **82**, 544–553 (1994).
5. A. Fukumoto, K. Aratani, S. Yoshimura, T. Udagawa, M. Ohta, and M. Kaneko, "Super resolution in a magneto-optical disk with an active mask," in *Optical Data Storage*, J. J. Burke, T. A. Shull, and N. Imamura, eds., *Proc. SPIE* **1499**, 216–219 (1991).
6. K. Torazawa, S. Sumi, S. Yonezawa, N. Suzuki, Y. Tanaka, A. Takahashi, Y. Murakami, and N. Ohta, "Key technologies to realize magneto-optical storage of over 7 Gbytes in a CD-sized disk," *Jpn. J. Appl. Phys.* **36**, 591–592 (1997).
7. H. Awano, S. Ohnuki, H. Shirai, N. Ohta, A. Yamaguchi, S. Sumi, and K. Torazawa, "Magnetic domain expansion readout for an ultra high density MO recording," *IEEE Trans. Magn.* **33**, 3214–3216 (1997).
8. K. Yasuda, M. Ono, K. Aratani, A. Fukumoto, and M. Kaneko, "Premastered optical disk by super resolution using rear aperture detection," *Jpn. J. Appl. Phys.* **32**, 5210–5213 (1993).
9. Y. Kasami, K. Yasuda, M. Ono, A. Fukumoto, and M. Kaneko, "Premastered optical disk by super resolution using rear aperture detection," *Jpn. J. Appl. Phys.* **35**, 423–428 (1996).
10. P.-Y. Liu and H.-P. D. Shieh, "Aperture/mask on magnetically induced super resolution readout," *J. Magn. Soc. Jpn.* **19s**, 339–342 (1995).
11. P.-Y. Liu and H.-P. D. Shieh, "Center aperture detection on magnetically induced super resolution magneto-optical disks," *J. Magn. Mag. Mater.* **155**, 385–388 (1996).
12. S. Yonezawa and H.-P. D. Shieh, "Laser pulse-readout on the detection of optical storage," Taiwan patent 107,340 (11 November 1995).
13. B.-W. Yang, W.-K. Hwang, and H.-P. D. Shieh, "Readout scheme by pulsed irradiation center aperture detection on magnetically induced super resolution magneto-optical disks," *Jpn. J. Appl. Phys.* **35**, 419–422 (1996).
14. N. Yamada, E. Ohno, K. Nishiuchi, and N. Akahira, "Rapid-phase transitions of GeTe–Sb₂Te₃ pseudobinary amorphous thin films for an optical disk memory," *J. Appl. Phys.* **69**, 2849–2856 (1991).
15. M. Mansuripur and G. A. N. Connell, "Laser-induced local heating of moving multilayer disks," *Appl. Opt.* **22**, 666–670 (1983).
16. T. Ohta, K. Inoue, M. Uchida, K. Yoshioka, T. Akiyama, S. Furukawa, K. Nagata and S. Nakamura, "Phase-change disk media having rapid cooling structure," *Jpn. J. Appl. Phys.* **28**, 123–128 (1989).
17. A. Yariv, *Optical Electronics* (Saunders, New York, 1991).
18. H. A. Macleod, *Thin-Film Optical Filters* (McGraw-Hill, New York, 1990).
19. J.-R. Liu and H.-P. D. Shieh, "Effects of initialization conditions on erasability of phase change optical disks," *IEEE Trans. Magn.* **34**, 435–437 (1998).